

Spin Correlations and Magnetic Order in Non-superconducting $\text{Nd}_{2-x}\text{Ce}_x\text{CuO}_4$

P. K. Mang¹, O. P. Vajk², A. A. Ivanitski², J. W. Lynn³, and M. G. Reven^{1,4}

¹Department of Applied Physics, Stanford University, Stanford, CA 94305

²Department of Physics, Stanford University, Stanford, CA 94305

³NIST Center for Neutron Research, National Institute for Standards and Technology, Gaithersburg, Maryland 20899 and

⁴Stanford Synchrotron Radiation Laboratory, Stanford, CA 94309

(Dated: January 29, 2020)

We report quantitative neutron scattering measurements of the evolution with doping of the Neel temperature, the antiferromagnetic correlations, and the ordered moment of as-grown, non-superconducting $\text{Nd}_{2-x}\text{Ce}_x\text{CuO}_4$ ($0 < x < 0.18$). The instantaneous correlation length is surprisingly well described by our quantum Monte Carlo calculations for the randomly site-diluted nearest-neighbor spin-1/2 square-lattice Heisenberg antiferromagnet. However, quantum fluctuations have a stronger effect on the ordered moment, which decreases more rapidly than for the quenched-disorder model.

PACS numbers: 74.25.Ha, 75.40.Mg, 75.50.Ee

Over the past eighteen years much has been learned about the evolution with doping of magnetic correlations in the high-temperature superconductors. For the prototypical material $\text{La}_{2-x}\text{Sr}_x\text{CuO}_4$ (LSCO), neutron scattering has led to the observation of the loss of long-range antiferromagnetic order and the concomitant decrease of two-dimensional (2D) spin correlations [1], an incommensurate spin-density wave [2], and coupled charge and magnetic "stripe" order upon co-doping with Nd [3]. The richness of the observed behavior is attributable to the evolution of the cuprate superconductors from Mott-insulating parent materials which are found to be excellent realizations, at low energies and long wavelengths, of the spin-1/2 square-lattice Heisenberg antiferromagnet (SLHAF) [4]. Although the vast majority of research has focused on the hole-doped systems, the electron-doped materials, typified by $\text{Nd}_{2-x}\text{Ce}_x\text{CuO}_4$ (NCCO) [5], have presented an important challenge to the field of high- T_c research and particularly to the paradigm established from experiments on LSCO. Unlike for LSCO, the magnetic phase of NCCO is very robust with respect to doping [6, 7, 8] and the magnetic correlations remain commensurate [8, 9].

Since superconductivity in the high- T_c cuprates appears in close proximity to antiferromagnetic phases, it is essential to understand the nature of nearby magnetic ground states. As-grown NCCO is not superconducting, and the antiferromagnetic phase extends to the highest concentration for which samples can be produced ($x < 0.18$). Oxygen impurities are believed to occupy the nominally vacant apical sites [10], and a relatively severe oxygen reduction procedure must be applied to induce superconductivity above $x = 0.13$ [5]. Although the reduction procedure weakens the magnetism, magnetic order is still observed near optimal doping where $T_c = 24$ K [11]. One qualitative argument often employed to explain the robustness of the antiferromagnetic phase in the electron-doped cuprates is that, whereas hole carriers are doped

into the $\text{O } 2p$ band and frustrate the antiferromagnetic arrangement of the neighboring Cu ions, doped electrons primarily reside on the Cu site, filling the 3d shell and removing the spin degree of freedom [6, 7, 8]. New, quantitative insights have been gained recently into the role of static non-magnetic impurities introduced into the spin-1/2 SLHAF [12, 13, 14, 15], and it would be interesting to test how well NCCO can be described by this model.

In this Letter, we present detailed neutron scattering results on the evolution with Ce doping of the magnetic properties of as-grown, non-superconducting NCCO ($0 < x < 0.18$). We find that the instantaneous spin correlations in the paramagnetic phase are, in effect, well described by the randomly-diluted spin-1/2 nearest-neighbor (NN) SLHAF model for which we have carried out numerical simulations. On the other hand, the ordered moment falls off more rapidly, a clear indication that quantum fluctuations are stronger than for the model magnet and that such fluctuations manifest themselves differently for different observables. We also find that the primary difference between the Neel temperature and ordered moment of as-grown and reduced NCCO is a shift in electron concentration that corresponds to $\delta x \approx 0.03$. Our result for the doping dependence of the ordered moment is in good agreement with recent theory for the one-band Hubbard model.

Crystals of $\text{Nd}_{2-x}\text{Ce}_x\text{CuO}_4$ were grown in 4 atm of O_2 using the travelling-solvent coating-zone technique. The solubility limit is about $x = 0.18$, and our study spans the range $0 < x < 0.18$. In addition, several samples were reduced for 20 h at 920 C in Ar followed by an anneal for 20 h at 500 C in O_2 for additional magnetic order parameter measurements. Magnetometry indicates that the reduced $x = 0.14$ and $x = 0.18$ samples are superconducting with $T_c = 24$ K and 20 K (onset), respectively. Our single-grain crystals are cylindrical, typically with a diameter of 4.5 mm, and range in volume from 0.1 to 0.7 cm^3 . Average Ce concentrations were verified

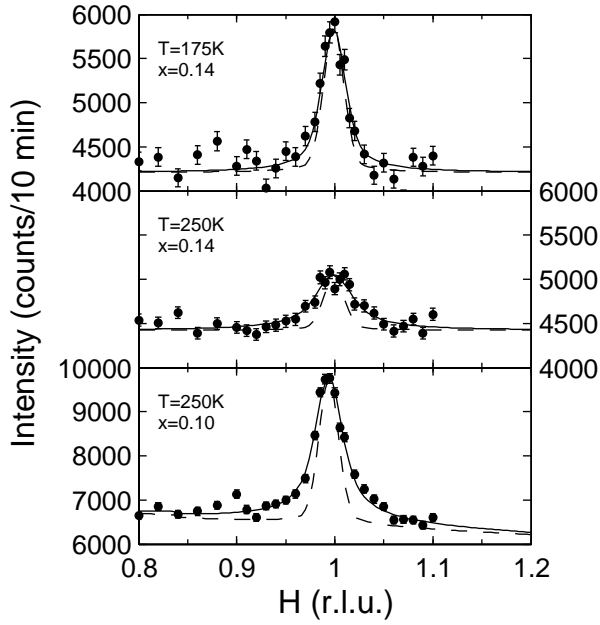


FIG. 1: Representative two-axis scans along $q_{2D} = (H=2, l=2; H=2, l=2)$ in the paramagnetic phase of $x = 0.10$ and 0.14 , with collimations $40^\circ-42.5^\circ$ -Sample- 23.7° and incident neutron energy $E_i = 14.7$ meV. The instrumental resolution is indicated by the dashed lines.

using inductively coupled plasma spectroscopy and typically found to equal the nominal values. The neutron scattering measurements were performed on the thermal triple-axis instruments BT 2 and BT 9 of the NIST Center for Neutron Research.

All as-grown samples exhibit long-range magnetic order at low temperature. However, significant two-dimensional (2D) magnetic correlations are already present well above the Neel temperature T_N . These may be probed through "two-axis" scans in which one integrates the dynamic structure factor $S(q_{2D}; \omega)$ over the limits set by the thermal energy, $k_B T$, and the incident neutron energy, E_i . If the integration is carried out over the relevant fluctuations one obtains the equal-time structure factor $S(q_{2D})$ [4]. In Fig. 1, we present representative scans of this type that show a peak in $S(q_{2D})$ at the incipient antiferromagnetic ordering wavevector. We fit these data to a 2D Lorentzian, $S(q_{2D}) = S(0)/(1 + q_{2D}^2 \xi^2)$, convolved with the instrumental resolution. As the temperature or the doping level is increased, correlations decrease, which is reflected in a broadening of the observed peaks.

Figure 2 summarizes the behavior of ξ/a for several Ce concentrations. Over a wide temperature range, the spin correlations exhibit an exponential dependence on inverse temperature, $\xi/a \sim \exp(2 \xi_s(x)/T)$ with spin stiffness $\xi_s(x)$, indicative of an underlying ground state with 2D antiferromagnetic order [16]. We overlay the results of quantum Monte Carlo simulations for the

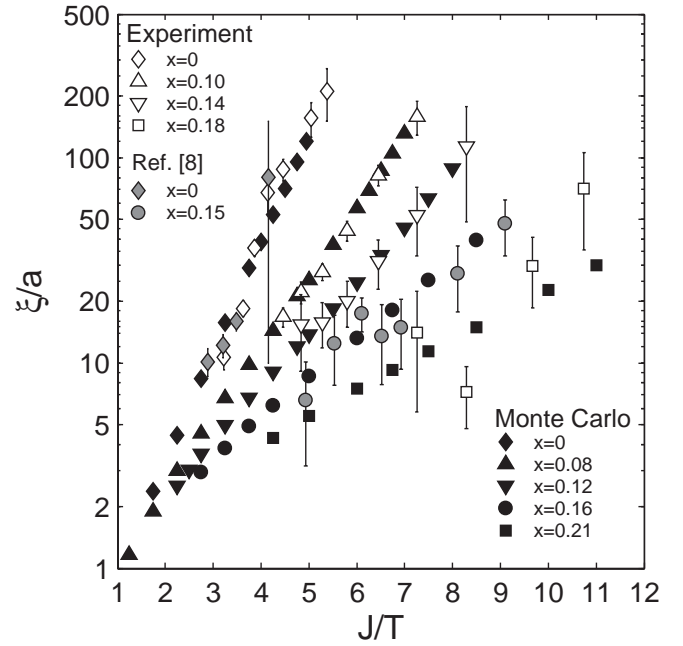


FIG. 2: Semi-log plot of the magnetic correlation length (in units of the lattice constant a) versus inverse temperature (in units of $J = 125$ meV) for $x = 0; 0.10; 0.14; \text{ and } 0.18$. The data terminate just above the onset of Neel order at low temperature. Also displayed are previous data for $x = 0$ and $x = 0.15$ [8] and Quantum Monte Carlo results for Eq. (1).

randomly-diluted SLHAF, described by the Hamiltonian

$$H = J \sum_{\langle i,j \rangle} p_i p_j S_i \cdot S_j; \quad (1)$$

where the sum is over NN sites, J is the antiferromagnetic Cu-O-Cu superexchange, S_i is the spin-1/2 operator at site i , $p_i = 1$ on magnetic sites, and $p_i = 0$ on nonmagnetic sites. The numerical method is the same as that employed previously [14]. The data are plotted as ξ/a , the ratio of the spin-spin correlation length to the NN Cu-Cu distance ($a = 3.95$ Å), versus J/T , the ratio of the NN antiferromagnetic superexchange of Nd_2CuO_4 to the temperature. A previous estimate from comparison of T_N with theory for the SLHAF yielded $J = 130$ meV [7], and we find $J = 125(4)$ meV from comparison with our numerical results for $x = 0$. Since the value of J has been established, the only adjustable parameter in the comparison for the Ce-doped samples is the concentration of nonmagnetic sites in Eq. (1). We find good qualitative agreement among experiment and Monte Carlo if we fix this concentration to equal the nominal Ce concentration x . However, as shown in Fig. 2, the agreement becomes quantitative if we allow the effective dilution to differ slightly: $x_e(x = 0.10) = 0.08(1)$, $x_e(x = 0.14) = 0.12(1)$, and $x_e(x = 0.18) = 0.21(2)$. Also shown are previous data for as-grown samples with $x = 0$ and $x = 0.15$ [8]. The

result for Nd_2CuO_4 agrees well with ours, and we estimate that x_e ($x = 0.15$) = 0.16 (2). The extent to which the quenched-disorder model Eq. (1) effectively describes the spin correlations of as-grown, non-superconducting NCCO is remarkable. The observed small differences between nominal electron concentration and effective static dilution may be in part due to the uncertainty in the oxygen (and hence electron) concentration of our samples. Another likely possibility is the presence of additional quantum fluctuations which are not captured in the effective Hamiltonian Eq. (1), for example due to frustrating next-NN interactions.

The spin stiffness of the disorder-free spin-1/2 NN SLHAF is known to be $2s_s J = 1.131(3)$ [17]. An estimate for the case of quenched disorder, Eq. (1), has been obtained in previous numerical work [14]. Comparison of the experimental results in Fig. 2 gives the effective values $2s_s J = 0.71(2)$, $0.54(4)$, $0.40(7)$, and $0.25(5)$, respectively, for $x = 0.10$, 0.14 , 0.15 , and 0.18 . The value $0.40(7)$ for the $x = 0.15$ sample is somewhat smaller than the original estimate of $2s_s J = 0.54$ [8] which was based on a classical rather than a quantum [14] picture for the doping dependence of the spin stiffness.

We note that Ref. [8] reports data for two as-grown $x = 0.15$ samples with onset of magnetic order at $T_N = 160$ and 125 K. If we allow for a distribution of Neel temperatures to account for the rounding of the observed transition, we estimate mean values of $T_N = 147(17)$ and $115(9)$ K, respectively. This is consistent with how we have treated our own data. The second sample from Ref. [8] also exhibits lower values of $\chi(T)$ (not shown in Fig. 2), comparable to our $x = 0.18$ crystal. The removal of apical oxygens through the reduction process changes both the degree of disorder and the carrier concentration. This lowers the Neel temperature and, for $x > 0.13$, leads to a decrease of the antiferromagnetic volume fraction and to bulk superconductivity [11]. Growth at lower oxygen partial pressure mimics the reduction process, resulting in lower oxygen contents and higher effective doping levels. The primary focus of this Letter is on non-superconducting, as-grown NCCO, and therefore we were careful to grow our samples under high oxygen partial pressure, resulting in crystals with T_N at or close to the maximum value attainable.

Figure 3(a) shows that the Neel temperature $T_N(x)$ of our as-grown samples, as obtained from neutron diffraction, approximately follows a parabolic form, extrapolating to zero at $x = 0.21$. As shown in Fig. 3(a), qualitatively similar behavior has previously been found for reduced NCCO for which $T_N(x)$ is lower [18]. The primary effect of the reduction is an approximately rigid shift of $j_x j_y = 0.03$ due to the change in carrier density. The convex doping dependence of NCCO is contrasted by the behavior exhibited by $\text{La}_2\text{Cu}_{1-x}(\text{Zn,Mg})_x\text{O}_4$ (LCZMO), for which Neel order extends up to the percolation threshold, $x_p = 0.41$; and the 2D spin correlations are quanti-

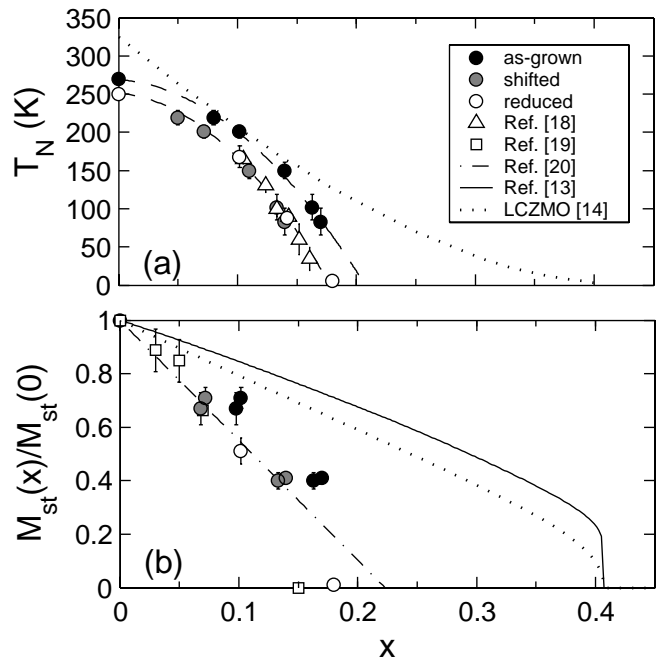


FIG. 3: (a) Neel temperature doping dependence. Ce-doped samples exhibit some rounding in the transition due to small oxygen and cerium inhomogeneities, which is represented by the error bars. The dashed curves are quadratic fits, and the dotted line indicates the behavior observed for LCZMO [14]. The grey circles are the as-grown data shifted by $j_x j_y = 0.03$. (b) Doping dependence of the ordered copper moment per site, normalized by the value for Nd_2CuO_4 . The grey circles are the as-grown data shifted by $j_x j_y = 0.03$. The open squares are data obtained in a previous study [19] and the dot-dashed line is a recent theoretical prediction for the one-band Hubbard model [20]. For comparison, Monte Carlo results for the diluted SLHAF (solid line) [13] and the behavior observed for LCZMO (dotted line) [14] are indicated as well.

tatively described by Eq. (1) up to x_p [14].

In Fig. 3(b), we plot the ordered moment for several samples, as obtained from order parameter measurements at low temperature. The values are normalized to that of Nd_2CuO_4 . Consistent with the behavior of $T_N(x)$, the moment of as-grown NCCO approaches zero much more rapidly than in the case of quenched disorder: at the rate $1 - M_{st}(x)/M_{st}(0) \approx 3.5x$ which is approximately twice that of the diluted SLHAF for $x < 0.20$: on the other hand, the magnetic phase extends much further than for LSCO [1] and Li-doped La_2CuO_4 [21], for which Neel order is destroyed above $x = 0.02$ and $x = 0.03$, respectively.

As shown in Fig. 3(b), the moment of reduced samples is lowered further. We note that these data are again normalized by the value for as-grown Nd_2CuO_4 , and that a rigid shift of $j_x j_y = 0.03$ leads to a good agreement of the two data sets. Our result furthermore is consistent with previous experimental work at lower concentrations [19]. The combined data in turn agree with a recent

theoretical prediction for the one-band Hubbard model [20, 22, 23]. This theory is based on an analysis of photoemission data for the evolution of the Fermi surface of $\text{Nd}_{2-x}\text{Ce}_x\text{CuO}_4$ ($0 < x < 0.15$) [24], and it argues in favor of a decrease of the effective on-site Coulomb repulsion $U(x)$ with doping. Since the theory extracts $U(x)$ as an input parameter from photoemission experiments performed on reduced samples, but does not take into account superconducting fluctuations, it pertains to reduced samples with $x < 0.13$ and, effectively, to as-grown $\text{Nd}_{2-x}\text{Ce}_x\text{CuO}_4$ up to higher doping. The good agreement therefore appears to support the assertion that the JM models are intrinsically limited in describing the electron-doped cuprates [20, 22, 25, 26, 27], and that a proper description requires the JM models with a decreasing value of U with increasing electron concentration [20, 22, 26, 27].

If viewed instantaneously, so as to mitigate the effects due to the increased itinerancy upon doping, the magnetism of NCCO should indeed resemble a system with quenched random site dilution. What is perhaps surprising is that for $(x; T)$ the correspondence with Eq. (1) is nearly quantitative. However, we note that recent theoretical developments indicate that our results for $(x; T)$ can also be understood in the context of the one-band Hubbard model [20, 27].

Since the charge carriers in as-grown NCCO are still fairly itinerant even well below T_N [28], deviations from the static model Eq. (1) can be expected to emerge as we view the two system on different time scales. Indeed, the ordered moment, an indicator of the strength of the magnetic order at infinitely long times, decreases much more rapidly in the case of as-grown NCCO than for the SLHAF. We note that slight deviations, possibly due to the presence of a frustrating next-NN exchange, are already observable for the ordered moment of LCZMO [14] (Fig. 3(b)), and that LCZMO is in close proximity to a new quantum critical point in an extended parameter space [15]. In the case of LCZMO, these perturbations are not quite strong enough to shift the critical point away from the geometric site-percolation threshold. Although the experimentally accessible doping range is limited, our results for as-grown NCCO are consistent with the existence of a quantum critical point below the geometric site-percolation threshold.

In summary, we present comprehensive neutron scattering measurements of the magnetic properties of non-superconducting $\text{Nd}_{2-x}\text{Ce}_x\text{CuO}_4$. Our data should serve as a benchmark for tests of still-emerging theories for the high- T_c phase diagram. Whereas the achievements of recent theoretical treatments of the Hubbard model are considerable, it is not clear at present if this model exhibits a superconducting ground state. Phonon anomalies have been observed in both electron and hole doped high-temperature superconductors [29], and a proper description of these materials may require the additional consideration of the electron-lattice coupling.

We acknowledge valuable discussions with N.P. Armitage, S. Larochelle, R.S. Markiewicz, M. Matsuda, and A.M.S. Tremblay, and thank I. Tanaka and the late H. Kojima for their invaluable assistance during the initial stage of the crystal growth effort. This work was supported by the US Department of Energy under Contracts No. DE-FG03-99ER45773 and No. DE-AC03-76SF00515, and by NSF CAREER Award No. DMR9985067.

-
- [1] B. Keimer et al., Phys. Rev. B 46, 14034 (1992), and references therein.
 - [2] K. Yamada et al., Phys. Rev. B 57, 6165 (1998), and references therein.
 - [3] J.M. Tranquada et al., Nature (London) 375, 561 (1995).
 - [4] R.J. Birgeneau et al., Phys. Rev. B 59, 13788 (1999).
 - [5] Y. Tokura, H. Takagi, and S. Uchida, Nature 337, 345 (1989).
 - [6] G.M. Luke et al., Phys. Rev. B 42, 7981 (1990).
 - [7] T.R. Thurston et al., Phys. Rev. Lett. 65, 263 (1990).
 - [8] M. Matsuda et al., Phys. Rev. B 45, 12548 (1992).
 - [9] K. Yamada, K. Kurahashi, Y. Endoh, R. J. Birgeneau, and G. Shirane, J. Phys. Chem. Solids 60, 1025 (1999).
 - [10] A. J. Schultz, J. D. Jorgensen, J. L. Peng, and R. L. Greene, Phys. Rev. B 53, 5157 (1996).
 - [11] T. Uefuji et al., Physica C 357-360, 273 (2001).
 - [12] S. Sachdev, C. Buragohain, and M. Vojta, Science 286, 2479 (1999).
 - [13] A.W. Sandvik, Phys. Rev. B 66, 024418 (2002).
 - [14] O.P. Vajk et al., Science 295, 1691 (2002); O.P. Vajk, M. G. Reven, P. K. Mang, and J. W. Lynn, Solid State Comm. 126, 93 (2003).
 - [15] A.W. Sandvik, Phys. Rev. Lett. 89, 177201 (2002); O.P. Vajk and M. G. Reven, Phys. Rev. Lett. 89, 172202 (2002).
 - [16] S. Chakravarty, B. I. Halperin, and D. R. Nelson, Phys. Rev. B 39, 2344 (1989).
 - [17] B. Beard, R. J. Birgeneau, M. G. Reven, and U.-J. Wiese, Phys. Rev. Lett. 80, 1742 (1998).
 - [18] T. Uefuji et al., Physica C 378-381, 273 (2002).
 - [19] M. Rosseinsky, K. Prassides, and P. Day, Inorg. Chem. 30, 2680 (1991).
 - [20] R.S. Markiewicz, cond-mat/0312594.
 - [21] T. Sasagawa et al., Phys. Rev. B 66, 184512 (2002).
 - [22] C. Kusko, R.S. Markiewicz, M. Lindroos and A. Bansil, Phys. Rev. B 66, 140513R (2002).
 - [23] Ref. [22] is a mean-field theory. Up to $x = 0.10$, quantum fluctuations lower $M_{st}(x)$ by $1 - 0.78 - 0.84$, so the ratio $M_{st}(x)/M_{st}(0)$ remains approximately unaltered. The linear behavior at higher concentrations is to be viewed as an upper bound [20].
 - [24] N.P. Armitage et al., Phys. Rev. Lett. 88, 257001 (2002).
 - [25] H. Kusunose and T.M. Rice, Phys. Rev. Lett. 91, 186407 (2003).
 - [26] D. Senchal and A.M.S. Tremblay, cond-mat/0308625.
 - [27] B. Kyung et al., cond-mat/0312499.
 - [28] The planar resistivity at 4.2 K is as low as $2 \text{ m}\Omega \text{ cm}$ for as-grown NCCO ($x = 0.15$): Y. Onose et al., Phys. Rev. Lett. 82, 5120 (1999).
 - [29] M. d'Astuto et al., Phys. Rev. Lett. 88, 167002 (2002), and references therein.